THE ASTROPHYSICAL JOURNAL, 221:788–796, 1978 May 1

NEAR-INFRARED LUMINOSITY-SENSITIVE FEATURES IN M DWARFS AND GIANTS, AND IN M31 AND M32

JUDITH G. COHEN
Kitt Peak National Observatory*
Received 1977 July 25; accepted 1977 November 3

ABSTRACT

Observations are presented of prominent near-infrared spectral features in M dwarfs and M giants which elucidate the behavior of these features (8183–8195 Å doublet of Na I, the Ca II triplet, 9910 Å FeH band, and TiO bands) as a function of luminosity and effective temperature. These spectral features have been measured from near-infrared spectra of the nuclei of M31 and M32. A luminosity function similar to that of the solar neighborhood is supported by our observations. Our measurements indicate an enhancement of metallicity in the nucleus of M31 as compared with that of M32.

Subject headings: galaxies: individual — galaxies: stellar content — infrared: spectra — luminosity function — stars: abundances

I. INTRODUCTION

The relative number of M dwarfs and M giants in external galaxies can be determined only by their contribution to the integrated light. This ratio is of great importance, as it affects the mass-luminosity ratio, missing mass in galaxies, and corrections to cosmological tests for evolution of galaxies. Attempts to measure luminosity-sensitive features in galaxy spectra, and thus separate M dwarfs from M giants, have been made by Spinrad and Taylor (1971), O'Connell (1976), Whitford (1977), and Frogel *et al.* (1975) with results gradually converging toward a normal luminosity function for the lower main sequence (i.e., no substantial dwarf enrichment). Recent improvements in detector technology have made the spectral region 0.8–1.0 μm much more accessible, and this is precisely the region where one may begin to expect the light from M-type stars to dominate that of the earlier-type stars. A study of the behavior in stars of luminosity-sensitive features in this spectral range will therefore be very useful in future attempts to synthesize the stellar content of galaxies from spectra. In this paper, we discuss the behavior of the outstanding near-infrared spectral features, namely, the 8183–8195 Å doublet of Na I, the infrared triplet of Ca II (8498, 8542, and 8662 Å), the TiO bands, and the FeH band (also known as the Wing-Ford band; Wing, Cohen, and Brault 1977) as a function of temperature and luminosity for M dwarfs and M giants based on a collection of high-dispersion spectra. We present observations of these features in M31 and M32 and interpret them with the aid of the simple model galaxies constructed by Whitford (1977). A method of separating metallicity variations from variations in the initial luminosity function is discussed. Our observations confirm that the nucleus of M31 is more metal-rich than that of M32, and in neither case is there substantial dwarf enhancement for the luminosity function in these galactic nuclei.

II. OBSERVATIONS

The spectra have been secured at various times over the 1976–1977 observing season with three different procedures. For most of the M giants and the two brightest M dwarfs, the coudé auxiliary telescope (plus a television guiding system) was used with the No. 5 camera of the 2.1 m coudé spectrograph with an RG-665 filter, a projected slit width of 25 μm, and the S-1 image tube cooled to $-40°$ C to obtain well-widened spectra on the baked IIIa-J emulsion at 20 Å mm^{-1} over the region 8000–9000 Å, and at 40 Å mm^{-1} over the region 0.92–1.0 μm. (These shall be denoted as Class A spectra.) Since the field of the image tube is 40 mm, a single exposure will reach from the Na I doublet to the Ca II triplet, and a separate exposure was taken for the FeH band. Exposure times for the bright giants were quite short, but for the only two M dwarfs accessible with this configuration, the exposures were about 1 hour, which is the maximum time for this system because of thermal background from the S-1 image tube.

Class B spectra were obtained by using the gold spectrograph on the 2.1 m telescope with the Nye lens as a camera and the cooled S-1 image tube (baked IIIa-J plates) as a detector. An RG-695 filter and a projected slit width of 30 μm were used with a dispersion of 85 Å mm^{-1} on a spectra 0.3 mm wide. Although the Nye lens is not ideal as a fast camera for the gold spectrograph, it does not appear to degrade significantly the resolution of the S-1 image tube and has the advantage of a suitable back focal distance. With this system (and the larger telescope aperture), M dwarfs with $V \leq 14$ were accessible in 45 minutes, and in 1 hour one could obtain untrailed

* Operated by AURA, Inc., under NSF contract AST 74-04129.

spectra of the nuclei of M31 and M32. A single spectrogram covered the whole region of interest from 0.8 to 1.0 μm.

To avoid the 1 hour limitation on exposure time caused by the thermal background of the cooled S-1 image tube, Class C spectra were obtained with an instrumental configuration the same as that described above for the Class B spectra with the exception of the detector, which was a 100 × 100 CID array cooled to liquid nitrogen temperature and mounted in a standard infrared Dewar. The CID detector (Aikens, Lynds, and Nelson 1976) was operated in an analog mode. It was linear to less than 1% up to 10,000 counts per pixel. The background was marginally detectable even after 2 hours. It can be operated continuously in a nondestructive read mode, and to reduce the readout noise, each picture was read 24 times. The pixel size was 60 μm × 80 μm, with the smaller side parallel to the spectrograph slit jaws so that a projected slit of 40 μm was used (with a dispersion of 83 Å mm^{-1} and an RG-695 filter). The profiles of Ar I comparison lines had FWHM of 1.5 pixels. The pictures are stored on magnetic tape for later processing. Because there are only 100 pixels, a single exposure will cover from the Na I doublet to the Ca II triplet if the grating is precisely centered. Because of some problems with centering, the usual range was from the Na I doublet to about 8600 Å, losing the last line of the Ca II triplet. A separate exposure centered at 9700 Å was taken. With this system, the spectra were untrailed, so that a stellar spectrum has a FWHM of about 3 pixels. Wolf 359 gave an exposure with a maximum of 350 counts per pixel along the pixel line where the stellar image was centered at 9900 Å in 30 min, or a total of about 800 counts per resolution element (i.e., per row) with the CID on the 2.1 m telescope. (This meant, in practice, that several bright galaxies were accessible in exposure times of less than 90 minutes.)

The CID pictures were processed by using software written by R. Lynds for the video camera. The spectrum occurred in 6–10 columns, depending on the seeing, centered on the array. Each picture was preceded by a "zero light" frame which was subtracted from the picture as the first step in processing. Because of small background effects, the mean level in the 90 columns with no spectrum was not zero, and a constant (always less than 20 counts) was added to the entire picture to make the mean background level zero. Then the pictures were divided by flat field exposures taken with an incandescent lamp and a sheet of Mylar over the grating.

The columns in which the untrailed spectrum occurred (usually between columns [50] and [60] were located, and the rows were averaged across the seeing disk using the count rate at row (50) of each column as the weight for the various columns. Unfortunately, this was only the third stellar run with the CID array, and some technical problems remain, so that the galaxy spectra, with a lower mean count rate, cannot be reduced with such a simple scheme; for the stellar spectra, the procedure described above gave satisfactory results. Stellar spectra of Classes A and B were measured with the PDS digital microphotometer and converted to intensity through calibration plates developed with the spectra by using standard techniques.

In Figure 1, we present intensity tracings of the Na I doublet from spectra of each class, while profiles of the 9910 Å FeH band are shown in Figure 2.

The most prominent stellar spectral features were measured on all the spectra, and the measurements are listed in Table 1. Three long-period variables were observed, and their phases (0.00 is maximum) are listed in parentheses. The values of $V - K$, which we use as a temperature index, are from Veeder (1974) for the M dwarfs. For the M giants, the $V - K$ values are from Johnson *et al.* (1966) or from the mean color for the spectral class based on Table 3A of Frogel *et al.* (1978). Only the supergiant has been

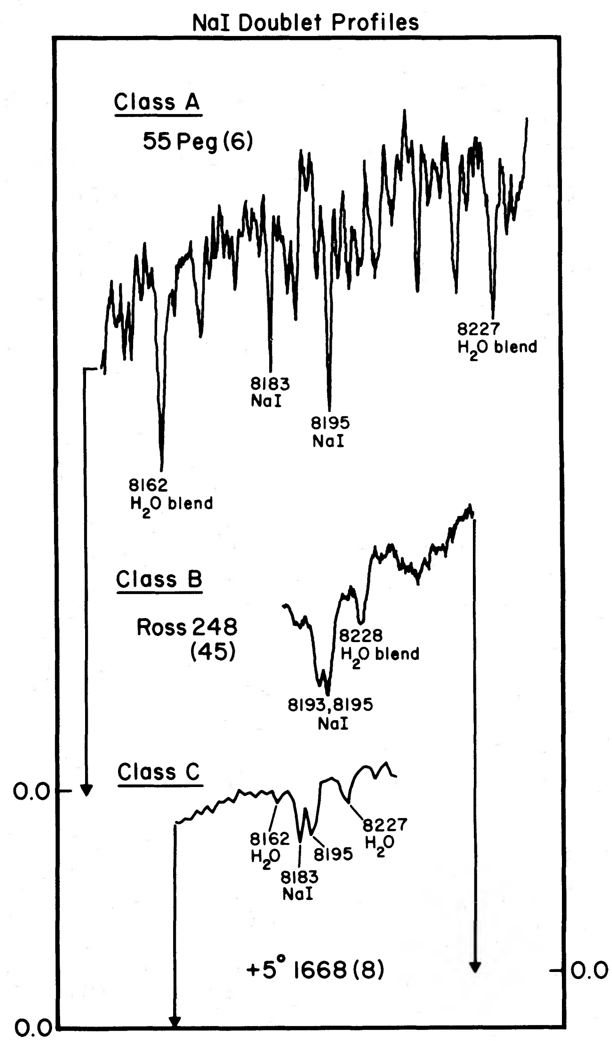

FIG. 1.—Intensity tracings of the region near the Na I doublet for representative spectra of Class A, B, and C. The zero-intensity position is indicated for each tracing. The number in parentheses after the name of the star is the exposure time in minutes.

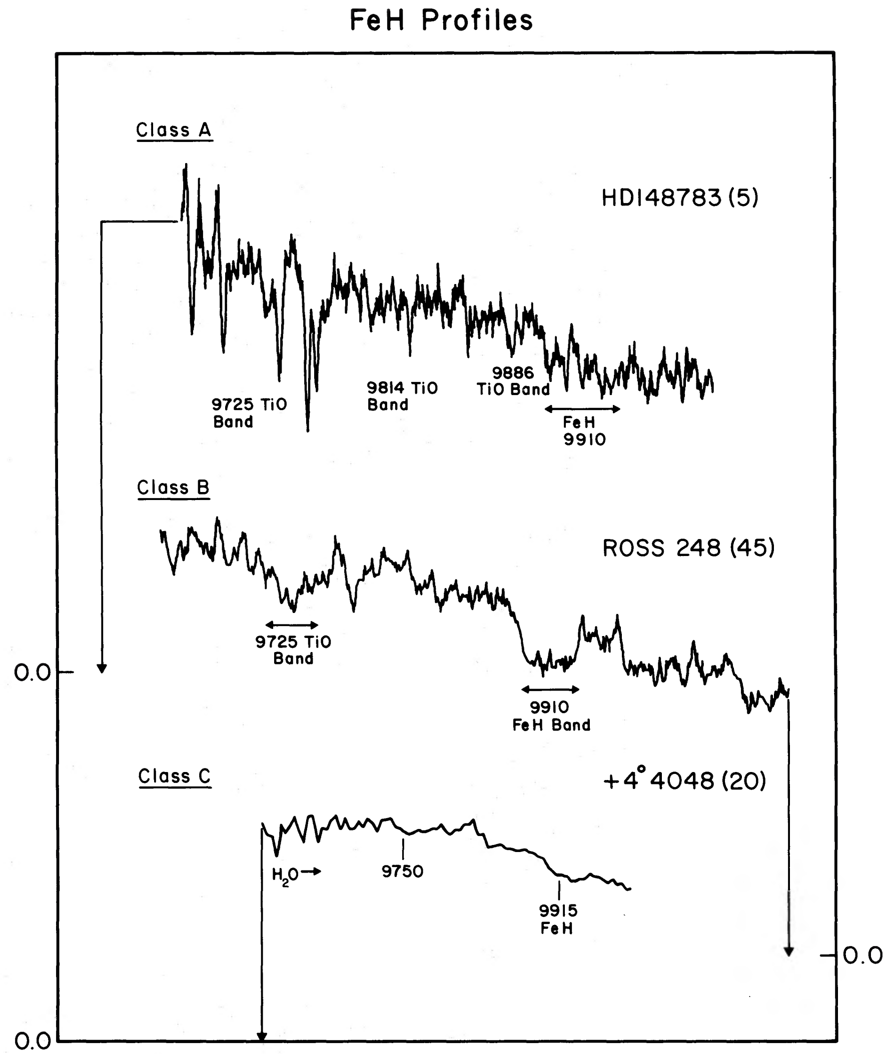

FIG. 2.—Intensity tracings of the region near the FeH band for representative spectra of Class A, B, and C. The zero-intensity position and exposure time are indicated as in Fig. 1.

corrected for reddening. $V-K$ for the three variables was assumed to be 9.0. The equivalent width W_λ of the two components of the Na I doublet is given in the third column for Class A and Class B spectra. For Class C spectra, only the total width of the two lines is given. The next set of columns contains W_λ for each line of the Ca II triplet. The next column displays the residual intensity of the 8430 Å TiO band at the wavelength 8490 Å (which does not coincide with the band head). The residual intensity of the Lockwood TiO bands (Lockwood 1973) with heads at 9725, 9814, and 9899 Å .were measured at 9750, 9820, and 9900 Å. Only the 9750 Å position was measured for the Class C spectra. The residual intensity at 9915 Å in the FeH band is in the final column. Note that the resolution of the Class A spectra is sufficiently great that the Na I doublet is detected in giants, the FeH band at 9910 Å has been seen for the first time in spectra of giants, and the 9899 Å TiO band is clearly separated from the 9910 Å FeH band. Because the bands of interest are broad even at the lowest dispersion used, and the Ca II and Na I lines are not resolved even at the highest dispersion, results are independent of different dispersions used. The errors are estimated as $\pm 3\%$ in residual intensity measurements and the maximum of 20% or ± 0.3 Å for the W_λ determinations, mostly owing to difficulties in determining the location of the continuum.

III. DISCUSSION OF THE STELLAR DATA

The behavior with temperature and luminosity of the near-infrared spectral features in M-type stars can now be determined. We use $V-K$ as a temperature index and plot the various measurements as a function of $V-K$ in Figure 3. Freehand curves are

TABLE 1

Measurements of Near-Infrared Spectral Features

	V-K	Sp. Class	Na I 8184-8198 (W_λ Å)	Ca II (W_λ Å) 8498	8542	8662	TiO (%) 8498	9725	9814	9886	FeH 9910 (%)
M Dwarfs											
+4°4048 (Gl 752)	4.47	1C	2.7	0.7	1.3	--	8:	6:	--	--	8
+45°2505 (Gl 661AB)	4.59	1C	2.4	0.6	1.2	--	10:	5:	--	--	9:
AD Leo (Gl 388)	4.83	3A	1.1+1.3	--	--	--	--	10	8	4	13
+5°1668 (Gl 273)	4.94	3A+1C	1.2+1.5	0.5	1.0	0.9	9	7	--	--	8:
Barnard's Star (Gl 699)	5.00	1B+1C	2.2+2.6	0.4	0.7	0.8	8	9	--	--	15
YZ CMi (Gl 285)	5.50	1C	4.8	--	--	--	--	7	--	--	18
Gl 83.1	5.64	1B	3.0+3.9	≤0.5	≤0.5	≤0.5	10	13	7	--	23
Ross 248 (Gl 905)	6.37	2B	2.2+2.9	≤0.5	≤0.5	≤0.5	16	11	5	--	15
UV Cet (A+B) (Gl 65)	6.70	1B	2.9+3.4	≤0.5	≤0.5	≤0.5	21	11	8	--	23
Wolf 359 (Gl 406)	7.44	1C	10.2	--	--	--	--	10	--	--	27
M Giants											
55 Peg	3.81	1A	0.3+0.4	1.5	3.0	3.0	6	2	≤ 2	≤ 2	3
μ Cep	4.11	1B	≤0.6+≤0.7	1.8	3.2	3.3	6	10	5:	--	≤ 3
9 Cnc	4.63	1C	≤0.3+≤0.3	1.4	3.2	2.7	≤ 5	--	--	--	--
HR 5299	5.34	2A	0.3+0.5	1.2	2.0	--	--	11	5	≤ 4	5
ρ Per	5.32	1A	0.2+0.2	1.1	1.9	2.2	5	11	5	3	4
χ Aqr	6.2	1B	≤0.2+≤0.2	1.4	2.6	2.4	13	6	--	--	≤ 4
71 Peg	6.2	1B	≤0.4+≤0.3	1.6	2.3	3.1	15	6	--	--	6:
18 Cep	6.2	1B	≤0.4+≤0.4	1.4	2.8	3.3	14	8	5	--	≤ 5
30 Her	7.02	1A	0.6+0.7	1.0	1.3	--	--	12	7	3	5
HD 207076	8	1A	0.4+0.4	--	0.6	0.6	63	18	12	10:	8:
R Aur (0.04)	9	1A	0.4+0.6	--	≤0.4	≤0.4	73	17	11	≤ 5	12
o Cet (0.88)	9	1A	≤0.2+≤0.2	≤0.4	0.4	0.6	50	10	4	≤ 2	≤ 2
R Cas (0.80)	9	1A	≤0.2+≤0.2	≤0.4	≤0.4	≤0.4	70	--	--	--	--

drawn through the points for dwarfs and giants. The sum of W_λ for the three lines of Ca II[1] shows the expected behavior of decreasing strength as the temperature decreases because all Ca is gradually going into the neutral state. The sharp increase of Ca II at all temperatures in the giants, as compared with the dwarfs, is a result of the lower pressures and higher ionization conditions prevalent in the giant-star atmospheres.

The sum of the W_λ for the two Na I lines shows the reverse effect in Figure 3*b*. As $V - K$ increases, Na becomes neutral and the lines become quite strong in dwarfs. In giants, the increased level of ionization and decreased pressure broadening keeps the Na I feature weak even for quite cool stars. This calibration of the strength of the Na I doublet fills in the very crude calibration given by Whitford (1977).

The residual intensity of TiO at 8490 Å and at 9750 Å is plotted in Figure 3*c* and 3*d*. There is no strong luminosity dependence for either of the TiO features, in agreement with the photometric system of Wing (Wing 1973; Wing, Dean, and MacConnell 1976), although O'Connell (1973) claims to detect an enhancement of TiO in late M giants. Therefore we interpret the variation in O'Connell's (1976) 8542 Å index as due to the strong enhancement of Ca II in giants and not to TiO. For the very late M-type stars with $V - K > 8$, the 8490 Å TiO measurement is very uncertain, as the TiO is extremely strong and the location of the continuum is uncertain. Note that the ratios of the strength of the three Lockwood bands measured are approximately 4:2:1. These ratios will be used in § IV to correct the galaxy FeH measurements for TiO blending.

The behavior of the 9910 Å FeH band is shown in Figure 3*c*, where the residual intensity at 9915 Å is plotted as a function of $V - K$. This is in good qualitative agreement with Whitford's (1977) calibration of his scanner data with a 32 Å bandpass. Furthermore, we confirm Whitford's (1977) measurement of the strength of FeH in late-type giants, and at the high dispersion of the Class A spectra, there is no problem of contamination by nearby TiO features. A theoretical discussion of the cause of luminosity sensitivity of the FeH band has been presented by Mould and Wyckoff (1978).

The metal abundances for the stars we have observed are not known. However, because the M dwarfs have both radial velocities and proper motions, their *UVW* velocities have been derived (Gliese 1969). Three of them (Gl 273, Gl 699, and Gl 905) have a component greater in magnitude than 50 km s^{-1}. Gl 905 also has a noticeably weaker Na I doublet and FeH band than is expected from its $V - K$ color, although it has normal $J - H$ and $H - K$ colors

[1] If not all the lines of the Ca II triplet were measured, the ratios of W_λ were assumed to be 1:2:2 for 8498, 8542, and 8662 Å, respectively.

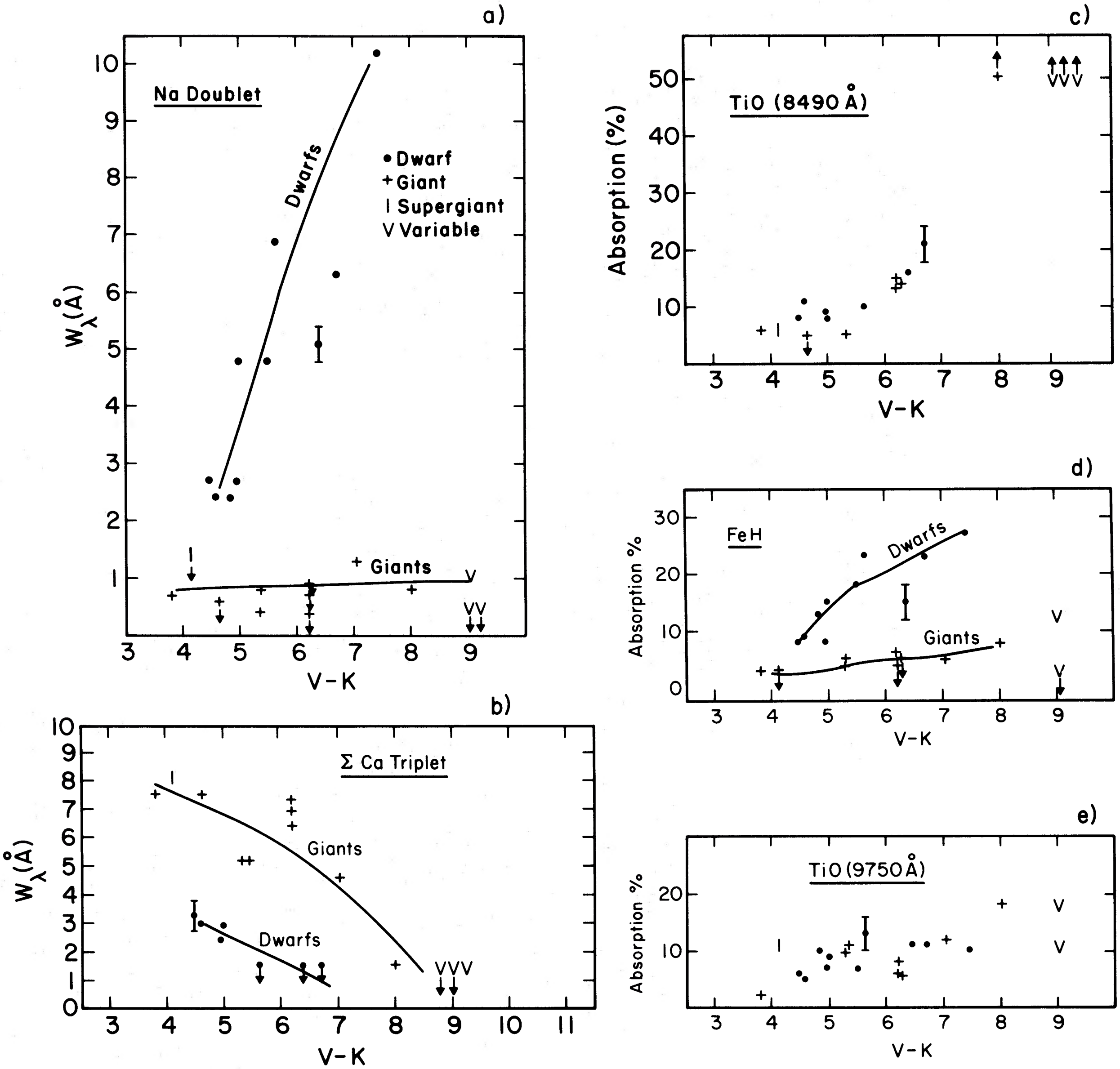

FIG. 3.—The observed strengths of the 8183–8195 Å Na I doublet, the Ca II triplet, TiO at 8490 Å, TiO at 9750 Å, and FeH at 9915 Å as a function of $V - K$. The solid points are dwarfs, the crosses are giants, the vertical bar is a supergiant, and the long-period variables are denoted by V. A freehand curve is drawn in some cases through the mean points for dwarfs and for giants. Error bars are indicated for one of the points in each panel.

(Persson, Aaronson, and Frogel 1978). We therefore tentatively find that Gl 905 is metal-poor, but assume that the rest of the calibrating stars of Table 1 are of solar metallicity.

IV. M31 AND M32

Three spectra of M31 and one of M32 were obtained with the gold spectrograph on the 2.1 m telescope with the S-1 image tube (Class B spectra). These spectra are untrailed, and only the nuclei gave a detectable result. A raster pattern using a 16 μm × 16 μm slit was traced around the spectra, and they were reduced using KPNO's Interactive Picture Processing System with software written by E. Jensen. In Table 2, we list the measured values for M32 and the average of the measurements for M31. The last column contains the FeH measurements corrected for the nearby Lockwood TiO band according to the ratios for the strength of the Lockwood TiO bands given in § III. Errors have been assigned on the basis of the scatter of the three values for M31. We note that the difference in the

TABLE 2

MEASUREMENTS OF NEAR-INFRARED SPECTRAL FEATURES IN M31 AND M32

	No. of Spectra (Class)	Na I 8183–8195 Å (W_λ)	Ca II 8498 Å (W_λ)	Ca II 8542 Å (W_λ)	Ca II 8662 Å (W_λ)	TiO 8498 Å (%)	TiO 9725 Å (%)	FeH 9915 Å (%)	FeH–TiO (%)
M31	3(B)	1.2A±0.3	---	2.9±0.5	2.2±0.4	5±3	8^{+2}_{-3}	7^{+2}_{-3}	5^{+2}_{-3}
M32	1(B)	0.3A±0.3	1.3±0.5	2.4±0.5	1.9±0.5	5±3	11^{+2}_{-4}	9^{+2}_{-5}	6^{+2}_{-4}

strength of the Na I doublet in M31 and M32 appears to be real. The reason for the discrepancy between our detection of FeH in M31 and Whitford's nondetection of FeH in several galaxies is not clear; however, Whitford's nondetection was very puzzling, as his mean galaxy measurement was less than his measurement of FeH even in giants, and at 9900 Å the contribution of the stars earlier than M0 to the integrated light is less than 50% even for $x = 0$ (Whitford 1977).

To evaluate the implications of these measurements, we use the simple galaxy model described by Whitford (1977). Although more sophisticated model galaxies can be concocted, Whitford's (1977) model is more than adequate, given the errors in the observations. This model has a single burst of star formation with a power-law initial mass function $dN(m)/dm = -(1 + x)$. In the solar neighborhood, Salpeter (1955) obtained $x = 1.35$, while Wielen's (1974) results for stars within 20 pc of the Sun show $x \approx 1.5$. Eggen (1976) has obtained a luminosity function for the galactic halo which agrees with that for the disk for stars earlier than M0, but has a greatly decreased number of M dwarfs in the halo. A possible variation of the initial mass function with metallicity in our Galaxy has been suggested by Da Costa (1977) from star counts in globular clusters. Spinrad and Taylor's (1971) dwarf-enriched model for the nucleus of M31 has $x \approx 2.5$. Therefore models are calculated for $0 \leq x \leq 3.4$.

The contribution to the integrated light in the continuum and in each spectral feature is calculated for 12 stellar types specified by Whitford (1977). The percentage of total luminosity at 9910 Å (L_{99}) given in Table 3 of Whitford (1977) has been appropriately corrected for each of the 12 spectral and luminosity groups to 8200 Å (L_{82}) (also used for the 8500 Å features) using the values of $R - I$ given by Johnson (1966). L_{99}, as tabulated by Whitford (1977), was used for the 9725 Å TiO band. The results of Figure 3, supplemented by the solar values (Moore, Minnaert, and Houtgast 1966) and those of α Boo (Mackle *et al.* 1975), were used to obtain W_λ or residual intensity for each group of stars contributing to the integrated light. In Table 3, we show the predicted strength of the various near-infrared spectral features for model galaxies as a function of x together with the measured values for M31 and M32. Although our predictions for the strength of the FeH band are slightly larger than those of Whitford (1977) owing to our larger observed strengths in late M dwarfs, we note that the FeH band is not as useful a discriminant as had been anticipated because it becomes really strong only in very late-type dwarfs, which do not contribute that much light, even at 0.99 μm, until $x > 3$. Therefore very accurate observations (±1%) will be necessary to determine x from the FeH band, and our observations do not achieve the required accuracy. The Na I doublet (determined from galaxy spectra, not from photometry) is much more suitable, as it becomes stronger in earlier M dwarfs than does FeH. The Ca II

TABLE 3

COMPARISON WITH WHITFORD'S MODEL GALAXY (SOLAR ABUNDANCES)

		$x = 0$	$x = 1$	$x = 2$	$x = 2.7$	$x = 3.4$	Observed M31	Observed M32	MMF
FeH (+TiO)	(%)	2	3	4	6	9	7^{+2}_{-3}	9^{+2}_{-5}	0.4
Na I Doublet	(Å)	0.7	0.8	1.1	1.7	2.1	1.2±0.3	0.3±0.3	0.4
TiO (8498 Å)	(%)	7	6	6	7	7	5±3	5±3	
TiO (9725 Å)	(%)	5	5	6	6	8	8^{+2}_{-3}	11^{+2}_{-4}	
Ca II (Sum of 3 lines)	(Å)	6.7	6.3	5.9	5.2	3.1	6.4±0.4	5.6±0.4	0.0* ≈0.2†

*theory
†observed

triplet is also a useful luminosity indicator sensitive to the presence of late-type giants, as O'Connell (1973) has emphasized.

Unfortunately, in addition to variations in the dwarf-to-giant ratio (i.e., x), we must consider possible variations in the metal abundance. Faber (1973*b*) and others have shown that nuclei of galaxies may be metal-rich as compared to the solar neighborhood, and that the metallicity enhancement is largest for the most luminous galaxies. Therefore we must estimate the effects of a possible enhancement of metallicity on the determination of x. We shall estimate crude metallicity multiplication factors (MMF listed in the last column of Table 3) for each observed spectral feature, such that the strength of a feature for any metallicity Z shall be $(Z/Z_\odot)^{\rm MMF}$. The MMF are estimated using the proportionality relationships given by Cayrel and Jugaku (1963) between the gas pressure P_g, the electron pressure P_e, $Z/Z_\odot$, the surface gravity g, assuming hydrogen-dominated atmospheres. The strength of FeH and Na I features are proportional to ZP_g/P_e, as they are strong only in late M-type stars where Na and Fe are predominantly neutral, while the strength of the Ca II triplet is taken to be proportional to ZP_g/P_e^2 for late-type giants. The gravity dependences thus derived for the Ca II triplet, Na I doublet, and FeH approximately match those of Figure 3. We therefore derive initial values of MMF which must be corrected for the change in line strength resulting from shifts toward cooler red giants and cooler main-sequence M dwarfs at a fixed bolometric magnitude as Z increases. Such corrections for a shift in effective temperature were made on the basis of the shift in the giant branch for globular clusters of various metallicities (Cohen, Persson, and Frogel 1978) and theoretical main-sequence calculations (Iben 1967). The changes in $T_{\rm eff}$ were converted to changes in $V-K$ and then to changes in line strength, using Figure 3. The final estimates of MMF are given in the last column of Table 3. No values are given for TiO, since we do not know the C/O ratio; however, the relatively good agreement of the computed and observed values for TiO is very comforting. These values of MMF will not hold for departures from solar metallicity greater than a factor of 4.

It is extremely desirable to verify observationally these theoretical MMF. Unfortunately, this is impossible for the Na I doublet or FeH, as abundances of M dwarfs are not available. For the infrared Ca II triplet, however, we have observed (Class A spectra) normal and extremely metal-poor K giants as well as K dwarfs. These data are summarized in Table 4. The $V-K$ values for the normal giants and dwarfs are from Johnson *et al.* (1966). For the metal-poor giants, $V-K$ is derived from the $T_{\rm eff}$ deduced from abundance analyses given by Sneden (1974) and from the calibration of $T_{\rm eff}$ versus $V-K$ of Cohen, Persson, and Frogel (1978). These observations demand that MMF (Ca II) ≈ 0.2 for metallicities below solar, and this may reasonably be assumed to hold for metallicities slightly larger. Therefore two values of MMF (Ca II) will be used for future calculations: the

TABLE 4

OBSERVATIONS OF K STARS (INFRARED Ca II)

	No. of Stars	Mean V-K	Mean Σ Ca II (infrared) (Å)
K0-K5 III	7	2.8	6.9
K0-K7 V	4	2.6	4.9
HD 122563 ([Fe/H]=-2.8)		2.6	2.2
HD 2665 ([Fe/H]=-1.6)		2.4	2.2:

theoretical value (0.0), and the observational one (0.2). With regard to TiO, assuming solar C/O, Mould and McElroy (1978) have shown that MMF (TiO) is positive. A definite value cannot be derived from their data.

Our basic strategy will be to use the value of x from Na I as compared with that from Ca II as a metallicity indicator. This is possible because, as x increases, the predicted Na I strength increases while that of Ca II decreases. Furthermore, because the Ca II lines are close in wavelength to the Na I doublet, the contribution to the integrated light of the galaxy by the various spectral and luminosity groups must be identical. If the metallicity is solar, the values of x derived from the Na I and Ca II features will agree. A metallicity enhancement will lead to x as derived from Na I being significantly larger than that from Ca II. A problem for the future is that of spectra for regions of galaxies with rotational velocities in excess of 250 km s^{-1}; there the use of atomic lines to determine metallicity and x will become more difficult because of the washing out of the lines owing to rotational broadening. Only molecular bands will be useful in these cases.

We now consider the case of M32. Here the best-determined observational values are TiO (8498 Å), Na I, and Ca II. Na I implies $x < 0$, while Ca II yields $2 < x < 2.7$. To resolve this inconsistency, we require a moderate metal deficiency. Consistency can be achieved with the observations for $x < 2$. Unless the metal deficiency is very large, however, $x > 1$ is suggested. The TiO and FeH values would then be at the lower limits quoted in Table 2; but considering the uncertainties in the data for M32, this is not a serious problem. Therefore, for M32, we find $1 \leq x \leq 2$ with a moderate metal deficiency as compared with the solar neighborhood.

For M31, the indices which increase as x increases (FeH and Na I) indicate large values of x ($x \geq 2$), while the one which decreases as x increases (Ca II) indicates a small value of x ($x \leq 2$). Therefore the nucleus of M31 must have either solar metallicity and $x \approx 2$, or more likely a metallicity slightly larger than the solar neighborhood and a value of x between 1 and 2. TiO stronger than predicted from our galaxy model would then be explained by the increased

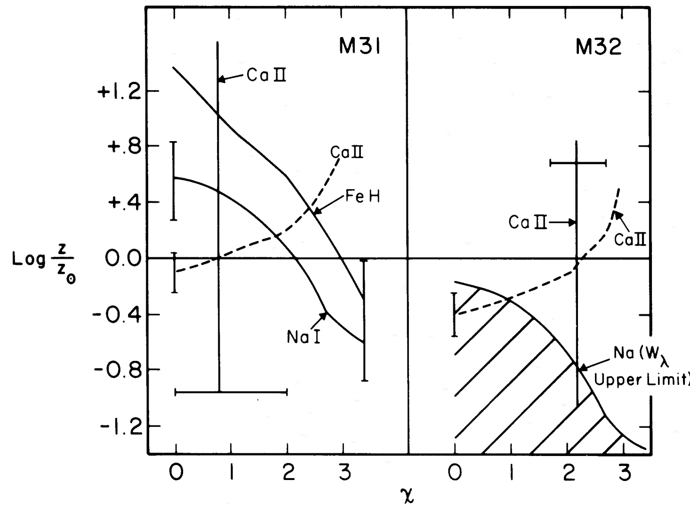

FIG. 4.—The value of metallicity ($Z/Z_{\odot}$) which fits the observations for each spectral feature in M31 and M32 as a function of x derived using the MMF of Table 3. The observational MMF for Ca II yields the dashed line. The errors along each curve are indicated at one point on each curve. The intersection of the various curves determines the metallicity and dwarf/giant ratio in each galaxy. For M32, the hatched region is that permitted by the observed strength of the Na I doublet.

metallicity. Values of x greater than 2.5 are not permitted for either M31 or M32. Since M32 is tidally limited (King 1962; Faber 1973*a*) and is intrinsically less massive than M31, it is not surprising that M32 has a lower abundance of metals in its nucleus than does M31.

The derivation of x and metallicity for M31 and M32 is presented in a more quantitative form in Figure 4. Here we use the MMF to derive the value of $Z/Z_{\odot}$ which will fit the observed strength for each spectral feature as a function of x. The highly uncertain FeH measurement for M32 is ignored here. Curves are shown for both the observational value of MMF (Ca II) and the theoretical value. The curves for Na I and FeH are not altered significantly by changes in MMF (Na I) of ± 0.1 for $x < 3$, because these features show a larger percentage of change in line strength in the range $0 < x < 3$ than does the Ca II infrared triplet. It is therefore fortunate that the most critical MMF is the one we have determined observationally. While the observational errors are large and our confidence in the estimates for MMF is small, Figure 4 clearly shows M31 more metal-rich than M32 with $1 \leq x \leq 2$ fitting the observations. If the MMF are approximately correct, M31 is metal-rich by a factor of 3 compared with the solar neighborhood, and M32 is more metal-poor by a factor which cannot be determined from present data. One should note that the suggestion of Peterson (1976) for selective enhancement of Na I in galactic nuclei may not be valid for M31, as the FeH band gives a similar metallicity enhancement, which is also suggested by TiO; but more observations are required for a definitive statement.

Whitford (1977) has discussed the other available data, such as the CO index (Frogel *et al.* 1975), the mean $V - K$ colors of galaxies (Frogel *et al.* 1978), and the mass-luminosity ratio (Faber and Jackson 1976) to demonstrate that they are all consistent with a giant-dominated population.

V. CONCLUSIONS

The near-infrared spectra of M-dwarf and M-giant stars obtained by us have elucidated the temperature and luminosity variations of the spectral features we have studied—the infrared Ca II triplet, the 8183–8195 Å Na I doublet, the 9910 Å band of FeH, and the 8430 Å and Lockwood bands of TiO. TiO has been shown to be independent of luminosity; the Ca II triplet is strongest in the giants and increases with increasing temperature, while the Na I and FeH features are stronger in dwarfs and decrease with increasing temperature. A method of separating metallicity variations from those of the initial luminosity function is suggested. Observations of the near-infrared spectral features in M31 and M32 have been presented which support an enhancement of metallicity in the nucleus of M31 as compared to M32, and $1 \leq x \leq 2$. Thus, a luminosity function similar to that of the solar neighborhood is supported by our observations. We can expect rapid progress in determining the luminosity function and metallicities of many galaxies as new array detectors become available. A theoretical analysis using spectral synthesis techniques to determine more accurately the multiplicity factors for metallicity enhancements in each near-infrared spectral feature would also be very useful.

We are grateful to J. A. Frogel for advice and suggestions during the course of this work and to R. Lynds and E. Jensen for help in picture processing techniques.

REFERENCES

Aikens, R. S., Lynds, C. R., and Nelson, R. E. 1976, *SPIE Proc.*, **78**, 65.
Cayrel, R., and Jugaku, J. 1963, *Ann. d'Ap.*, **26**, 495.
Cohen, J. G., Persson, S. E., and Frogel, J. E. 1978, *Ap. J.* (to be published).
Da Costa, G. 1977, Ph.D. thesis, Australian National University.
Eggen, O. J. 1976, *Ap. J. Suppl.*, **30**, 351.
Faber, S. M. 1973*a*, *Ap. J.*, **179**, 423.
———. 1973*b*, *Ap. J.*, **179**, 731.
Faber, S. M., and Jackson, R. E. 1976, *Ap. J.*, **204**, 668.
Frogel, J. A., Persson, S. E., Aaronson, M., Becklin, E. E., Matthews, K., and Neugebauer, G. 1975, *Ap. J.* (*Letters*), **195**, L15.
Frogel, J. A., Persson, S. E., Aaronson, M., and Matthews, K. 1978, *Ap. J.*, **220**, 75.
Gliese, W. 1969, *Veröff. Heidelberg No. 22* (*Catalogue of Nearby Stars*).
Iben, I., Jr. 1967, *Ann. Rev. Astr. Ap.*, **5**, 571.
Johnson, H. L. 1966, *Ann. Rev. Astr. Ap.*, **4**, 193.
Johnson, H. L., Mitchell, R. I., Iriarte, B., and Wisniewski, W. B. 1966, *Comm. Lunar Planet. Lab.*, **4**, 99.
King, I. R. 1962, *A.J.*, **67**, 471.
Lockwood, G. W. 1973, *Ap. J.*, **180**, 845.
Mackle, R., Griffin, R., Griffin, R., and Holweger, H. 1975, *Astr. Ap. Suppl.*, **19**, 303.
Moore, C. E., Minnaert, M. G. J., and Houtgast, J. 1966, NBS Monograph 61.
Mould, J. R., and McElroy, D. B. 1978, *Ap. J.* (to be published).
Mould, J. R., and Wyckoff, S. 1978, *M.N.R.A.S.*, in press.
O'Connell, R. F. 1973, *A.J.*, **78**, 1074.
———. 1976, *Ap. J.*, **206**, 370.
Persson, S. E., Aaronson, M., and Frogel, J. A. 1978, *Ap. J.*, in press.
Peterson, R. C. 1976, *Ap. J.* (*Letters*), **210**, L123.
Salpeter, E. E. 1955, *Ap. J.*, **121**, 161.
Sneden, C. 1974, *Ap. J.*, **189**, 493.
Spinrad, H., and Taylor, B. J. 1971, *Ap. J. Suppl.*, **22**, 445.
Veeder, G. J. 1974, *A.J.*, **79**, 1056.
Whitford, A. E. 1977, *Ap. J.*, **211**, 527.
Wielen, R. 1974, in *Highlights of Astronomy*, ed. G. Contopoulos (Dordrecht: Reidel), **3**, 395.
Wing, R. F. 1973, *Variable Stars in Globular Clusters and Related Systems*, ed. J. D. Fernie (Dordrecht: Reidel), p. 164.
Wing, R. F., Cohen, J. G., and Brault, J. 1977, *Ap. J.*, **216**, 659.
Wing, R. F., Dean, C. A., and MacConnell, D. J. 1976, *Ap. J.*, **205**, 186.

JUDITH G. COHEN: Kitt Peak National Observatory, P.O. Box 26732, Tucson, AZ 85726